Polarimetric observations with the Ringo polarimeter at the Liverpool Telescope

Agnieszka Słowikowska

Institute of Astronomy, University of Zielona Góra, Poland

2015, Sep 21th

In collaboration with

Krzysztof Krzeszowski	IA UZ
Michał Żejmo	IA UZ
Pablo Reig	FORTH/Uni. of Crete
Roberto Mignani	MSSL / UCL / IA UZ

Maximum observed and expected degree of polarisation

Radio	
galactic continuum	70%
quasars (integrated / resolved)	15% / 70%
Crab nebula	30%
pulsars (linear / circular)	80% / 70%

Optical	
planets	$>$ 20%
interstellar dust acting on starlight (linear)	10%
interstellar dust acting on starlight (circular)	0.05%
Sun and A_p stars (Zeeman effect)	100%
white dwarfs (Zeeman effect)	12%
symbiotic stars (Raman scattering)	8%
reflection nebulae (including Herbig–Haro and bipolar	60%
post–AGB stars and proto–PN (global polarisation)	30%
synchrotron (Crab nebula, blazars)	50%
synchrotron (extragalactic jets)	20%
Crab pulsar	10%

X–ray (mainly 'expected')	
solar flares	5%
Crab nebula	15%
accreting X–ray pulsars	80%
rotation–powered X–ray pulsars	10%
black hole (Lense–Thirring effect Cyg X–1)	2%
active galactic nuclei	20%
Seyfert accretion disc reprocessing	5%

γ–ray ('expected')	
pulsars	100%

GASP and AquEYE & IquEYE

GASP – Galway Astronomical Stokes Polarimeter

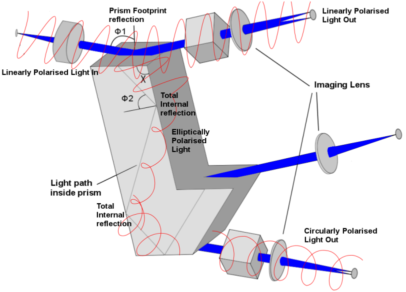

Andy Shearer (NUI, Galway)

AQuEYE and IQuEYE

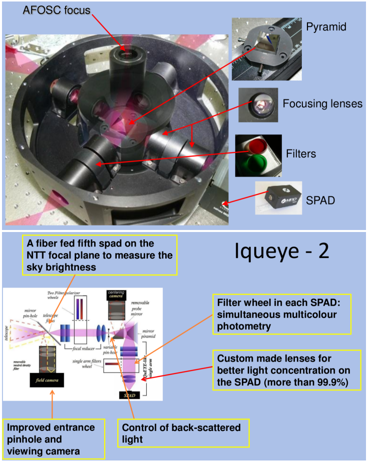

Cesare Barbieri (University of Padova)

Optical Pulsar TIMing Analyzer [1]

1.3m telescope at Skinakas

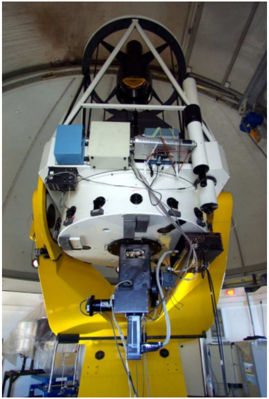

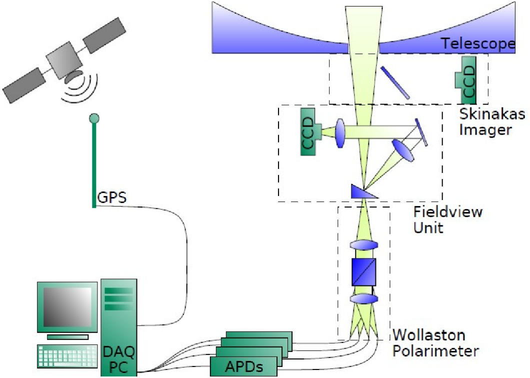

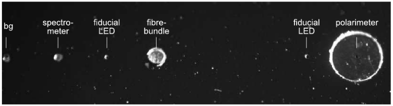

(a)

(b)

[1] http://www.mpe.mpg.de/OPTIMA

The Fermi Large Area Telescope gamma-ray Pulsar Catalog

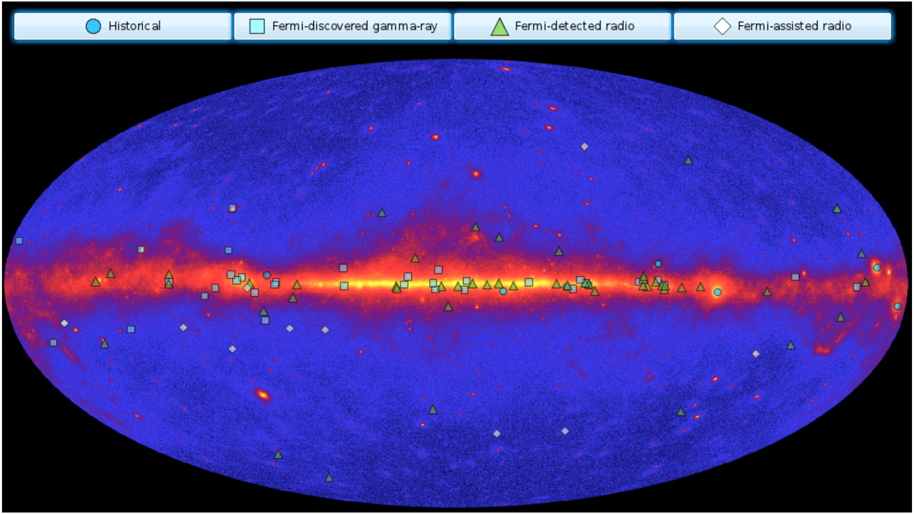

https://confluence.slac.stanford.edu/display/GLAMCOG/Public+List+of+LAT-Detected+Gamma-Ray+Pulsars

H–R diagram for pulsars (P–$\dot{P}$)

$$\dot{E} \propto \dot{P} P^{-3}$$

$$B \propto \sqrt{P \dot{P}}$$

$$\tau \propto P \dot{P}^{-1}$$

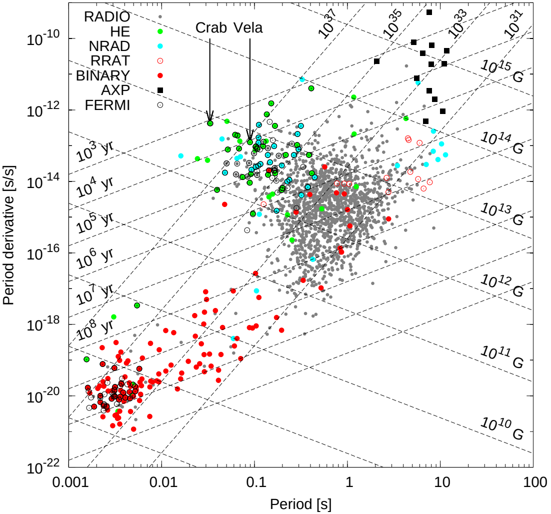

UV, O, IR observations of pulsars

Name	Year	Age	mag	D(kpc)	A_V	Phot	Spec	Pol	Tim	Astrom
pulsars										
Crab	1969	3.10	16.5	1.73	1.6	UVOIR	Y	Y	P	PM
B1509-58	2000	3.19	26	4.2	5.2	OIR		UL*		
B0540-69	1984	3.22	22	49.4	0.6	OIR	Y	Y*	P	PM (UL)
Vela	1976	4.05	23.6	0.23	0.2	UVOIR	Y	Y*	P	PM,PAR
B0656+14	1988	5.05	25	0.29	0.09	UVOIR	Y	Y	P	PM
Geminga	1984	5.53	25.5	0.16	0.07	UVOIR	Y		P	PM,PAR
B1055-52	1997	5.73	24.9	<0.72	0.22	UVO				PM
B1929+10	1996	6.49	25.6	0.33	0.15	UV				PM
B0950+08	1996	7.24	27.1	0.26	0.03	UVO				
B1133+16	*2008*	*6.69*	*28*	*0.35*	*0.12*	*O*				
J0108-1431	*2008*	*8.3*	*27.*	*0.3*	*0.05*	*O*				
J0437-471	2004	9.20		0.14	0.11	UV	Y			
XDINSs										
J1308.6+2127	2002	6.17	28.6	<1	0.14	O				
J0720-3125	1998	6.27	26.7	0.35	0.10	O				PM,PAR
J1856-3754	1997	6.60	25.7	0.14	0.12	O	Y			PM,PAR
J1605.3+3249	2002	-	26.8	<1	0.06	O				PM
RBS1774	2008	-	27.4	<0.5	0.2	O				
J0806-4123	2011	>6.5		<0.5		O				
magnetars										
SGR1806-20	2004	3.14	20.1	15	29	IR				
1E 1547.0-5408	2009	3.14	18.5	9	17	IR		Y*		
1E 1048.1-5937	2004	3.63	21.3	3	6.1	OIR		UL*	P	
XTE J1810-197	2004	3.75	20.8	4	5.1	IR		UL*		
SGR 0501+4516	2009	4.1	19.1	~2	5	IR			P	
4U 0142+61	2002	4.84	20.1	>5	5.1	OIR			P	
1E 2259+586	2002	5.34	21.7	3	5.7	IR				

*** phase-averaged**

10 PSRs identified, plus 2 candidates, mostly in the optical, 8 also in the nUV and 6 also in the nIR,

low-res spectroscopy for 5 PSRs only

Phase resolved Crab pulsar polarimetry

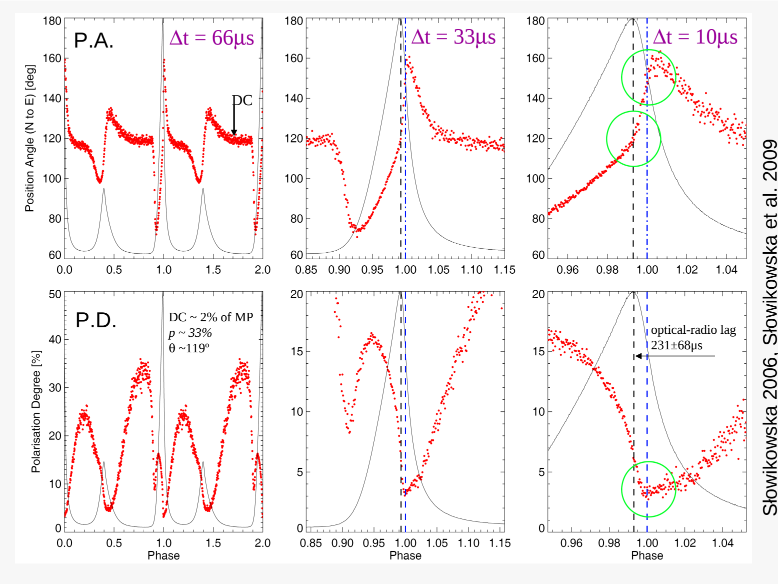

Decomposition of the optical polarisation components of the Crab pulsar and its nebula (OPTIMA vs. HST/ACS)

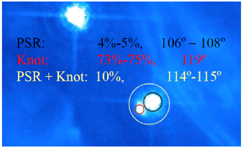

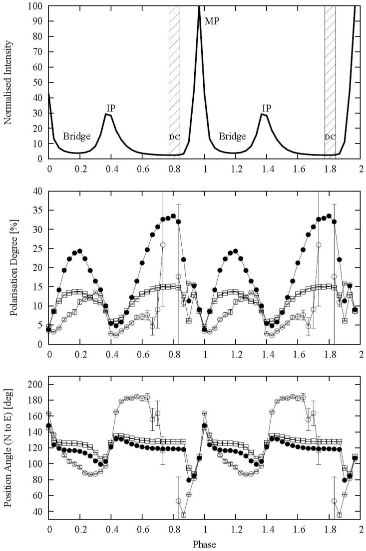

Left: HST/ACS Stokes I map of the Crab nebula and pulsar. **Right:** Top panel: the Crab pulsar light curve (MP, IP, bridge as well as the DC region: 0.78–0.84). Middle and bottom panels show the PD and PA (N to E) as a function of pulsar rotational phase, respectively. Three cases are shown:

- all sources of emission are taken into account, i.e. nebula, pulsar and the DC component - marked with the open squares symbols;
- the nebula contribution was subtracted by averaging the Stokes parameters in the hexagonal ring fibres - marked with black filled circles;
- assuming the constant PD and PA component during the DC phase we subtracted corresponding Stokes parameters to obtain pure pulsar polarisation characteristics as its rotational phase (open circles).

Cases 1-3 show the influence of separated components to the polarisation characteristics, also in the case if one calculates the phase-averaged PD and PA. (Słowikowska et al. 2012)

Comparison of optical measurements of two–pole caustic, polar cap and outer gap models

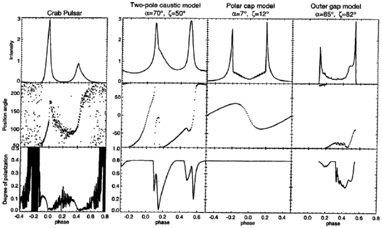

Dyks, Rudak & Harding 2004

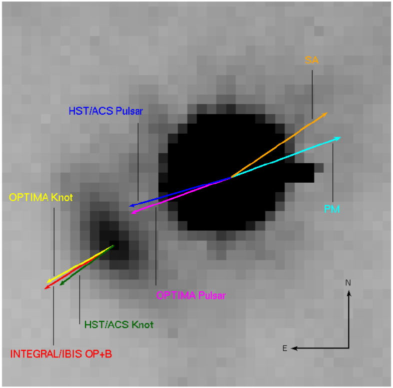

Moran et al. 2013, arXiv: 1305.6824

Recent X-ray polarimetry of the Crab pulsar:
Dean et al. 2008, Integral/SPI, 100 keV - 1 MeV, DC: PA=123±11 deg, PD=46±10 %
Forot et al. 2008, Integral/IBIS, 200 - 800 keV, DC: PA=120.6±8.5 deg, PD > 72 %

Weisskopf et al. 1978, 2.6 - 5.2 keV, the whole Crab nebula, PD=19.2±1.0 %

High time resolution measurements of the polarization of the Crab pulsar at 1.38 GHz

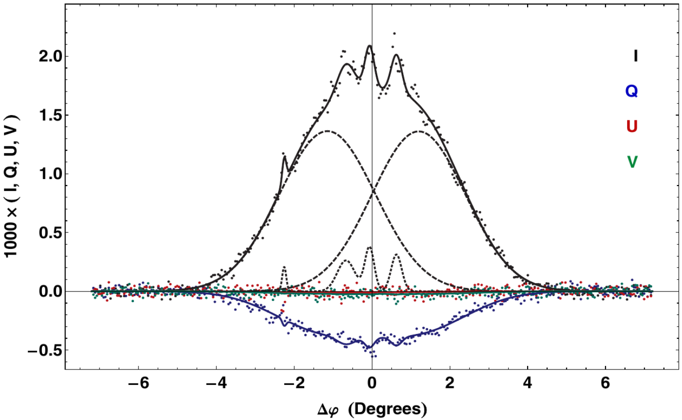

Słowikowska et al., 2015

High time resolution measurements of the polarization of the Crab pulsar at 1.38 GHz

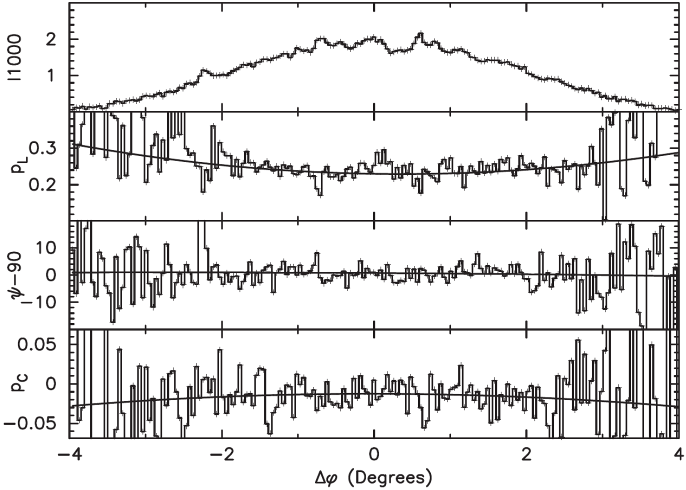

Słowikowska et al., 2015

Optical circular polarization of the Crab pulsar with the GASP at the WHT in December 2015

GASP – Galway Astronomical Stokes Polarimeter

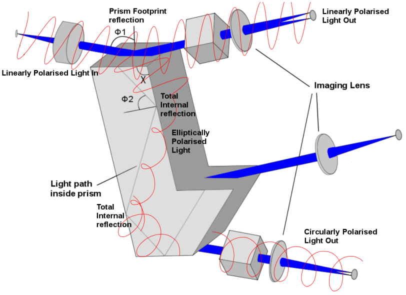

4.2-m William Herschel Telescope

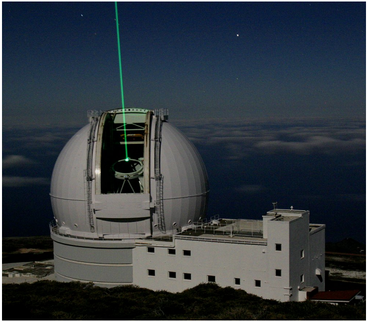

Andy Shearer (NUI, Galway)

The fractional polarization as a function of $\dot{E}$, Weltevrede and Johnston 2008

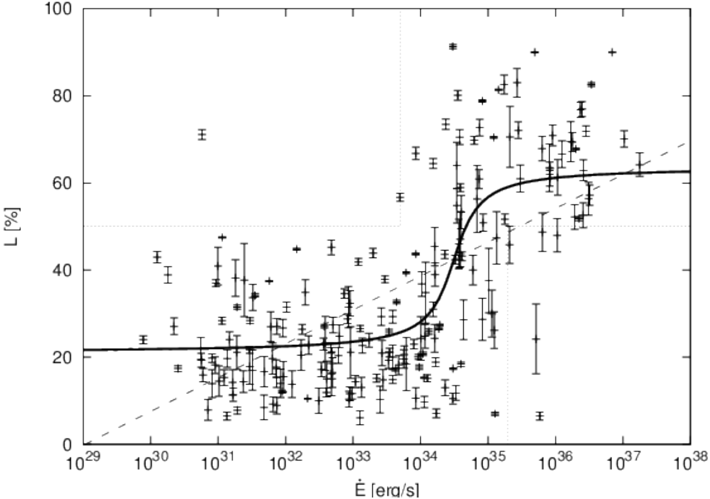

Phase averaged polarization degree [%] as a function of τ, P, $\dot{P}$ and $\dot{E}$ (Mignani et al. 2015)

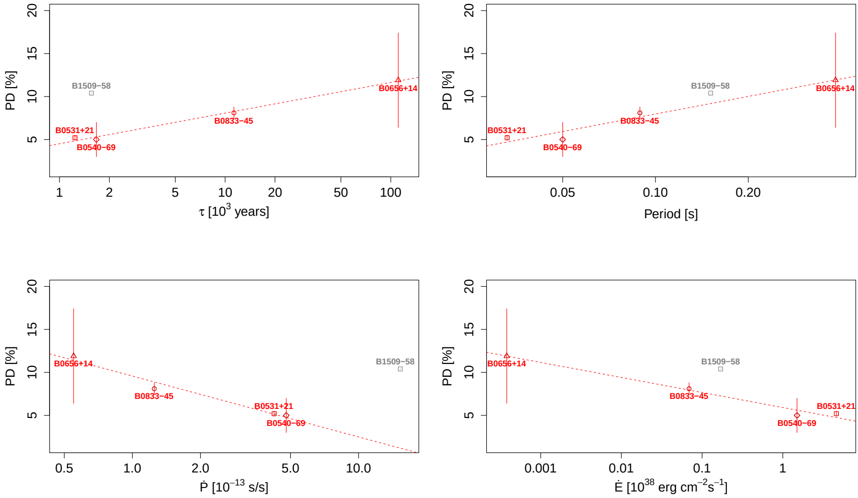

Phase averaged polarization degree [%] as a function of B_s, B_{lc}, Dist and DM (Mignani et al. 2015)

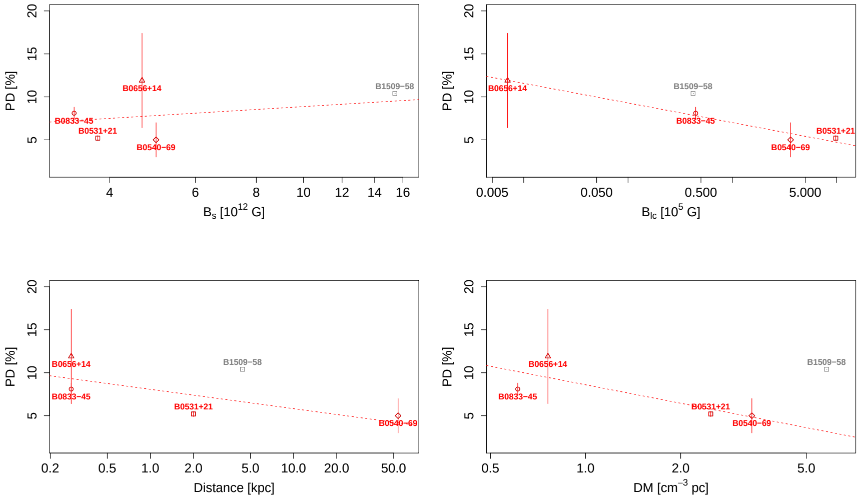

Phase averaged polarization of the Vela pulsar
PD $= 9.4\% \pm 4.0\%$

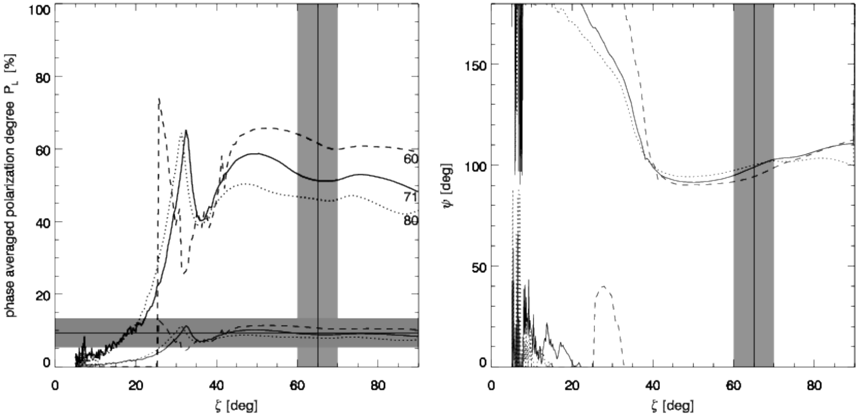

We assume $\alpha = 71^\circ$ as a representative value (Mignani et al. 2007).

Classification of high mass X-ray binaries

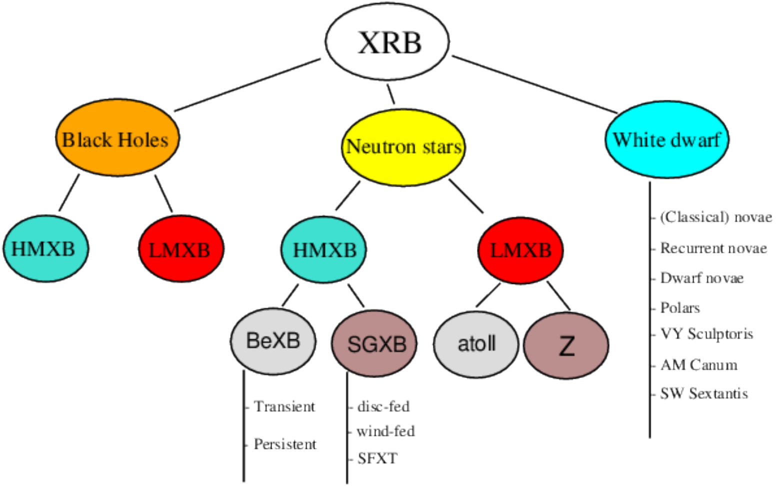

P. Reig 2011

P_{spin} vs. P_{orb} diagram of BeXBs

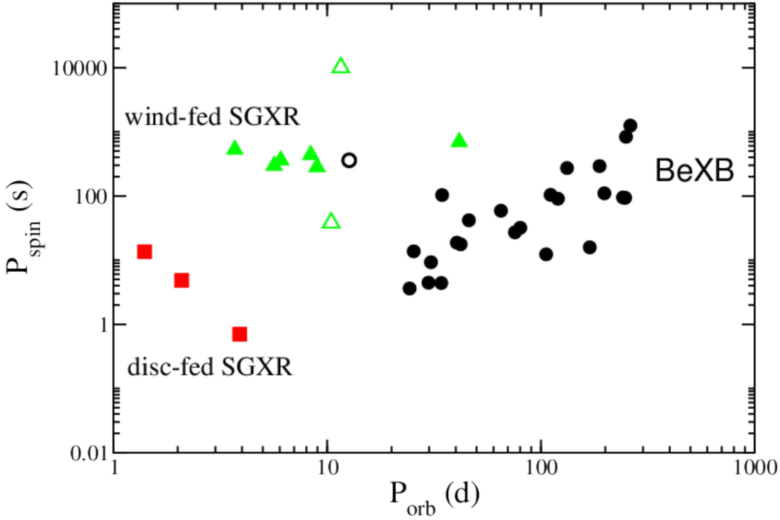

P. Reig 2011

RoboPol – photopolarimeter designed specifically for the 1.3-m telescope at the Skinakas Observatory, Crete, Greece

Instrument A. N. Ramaprakash (IUCAA), PI: O.G. King (Caltech)

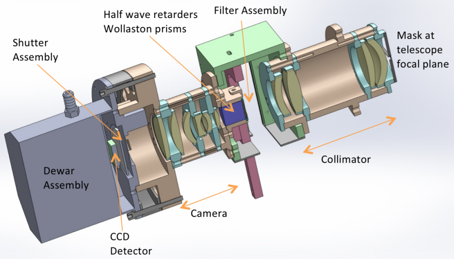

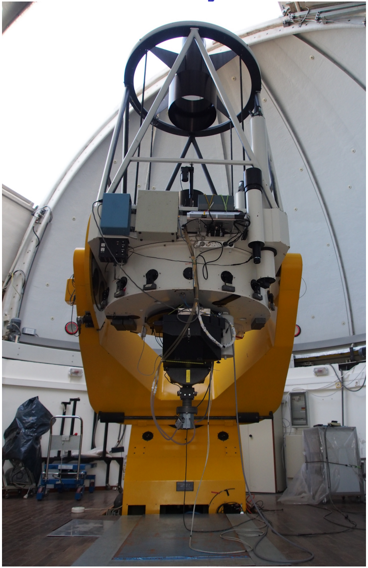

robopol

http://www.robopol.org

Pablo Reig's talk on RoboPol (Wednesday, 10:30–10:50)

RoboPol

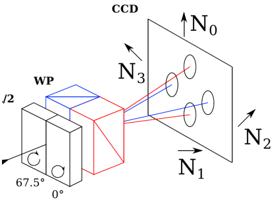

$$q = \frac{N_0 - N_1}{N_0 + N_1} \qquad u = \frac{N_2 - N_3}{N_2 + N_3}$$

Actual RoboPol image

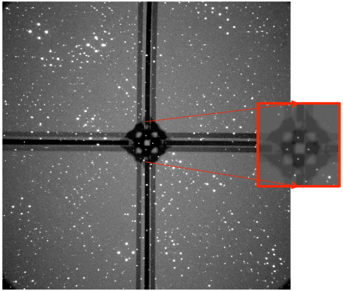

A focal plane mask blocks an area around the center of the field. This ensures maximum sensitivity for the central target by limiting the sky background in the center of the field.

Systematic errors are well-constrained. After calibration systematics are:

- *q* and *u*: < 0.1%
- Photometry: < 1%

`http://www.robopol.org` Pablo Reig's talk on RoboPol (Wednesday, 10:30– 10:50)

RoboPol measurements of selected BeXBs and the Crab pulsar

source	PD [%]	PA [deg]	V mag	exposure time
SAX J2103.5+4545	1.89±0.26	-2.4±4.0	13.8–14.4	30 sec x 6
V 0331+530	3.78±0.50	-58.8±3.8	15.1–15.8	68 sec x 2
4U 0115+634	3.7±0.3	-66.9±2.2	14.8–15.5	30 sec x 6
IGR J21342+4738	0.9±0.4	32.8±11.2	14.1	37 sec x 3
GRO J2058+40	4.0±0.3	65.8±2.0	14.9	25 sec x 6
KS 1947+300	2.5±0.3	22.7±3.4	14.1–14.2	60 sec x 2
KS 1947+300	2.6±0.4	15.5±4.5	14.1–14.2	31 sec x 3
Crab pulsar	5.56±0.74	111.1±3.8	16.6	200 sec x 3

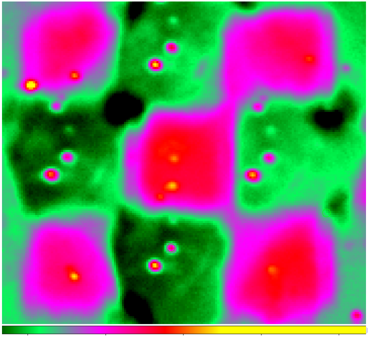

RINGO3 – polarimeter on the 2.0-m Liverpool Telescope

RINGO3 is a fast-readout imaging optical polarimeter. It uses a polaroid that rotates once per second to polarise signal going into a set of dichroics mirrors that split the beam into three:

– blue: 350-640 nm,
– green: 650-760 nm,
– red: 770-1000 nm,

for simultaneous polarised imaging in three wavebands with three separate cameras.

`http://telescope.livjm.ac.uk/Info/TelInst/Inst/RINGO3/`

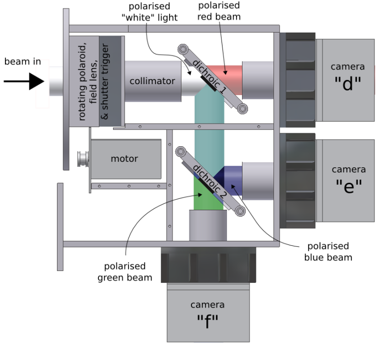

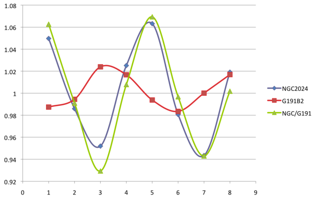

LT/RINGO3, G191B2B

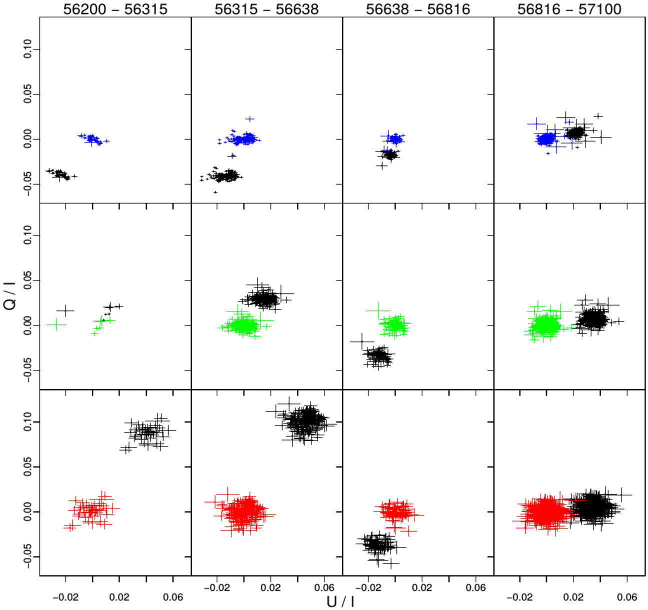

LT/RINGO3, G191B2B

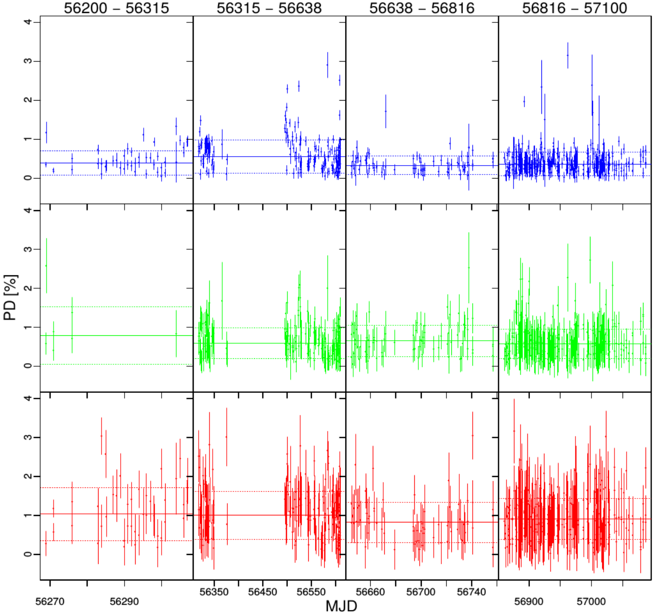

LT/RINGO3, BD +64 106

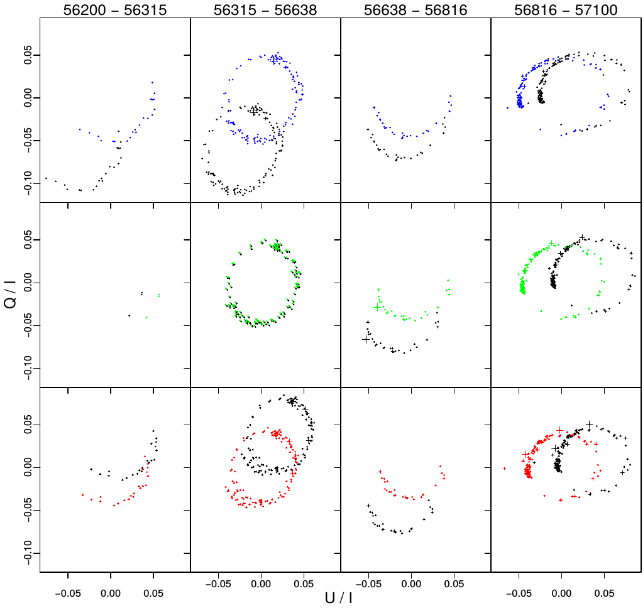

LT/RINGO3, BD +64 106

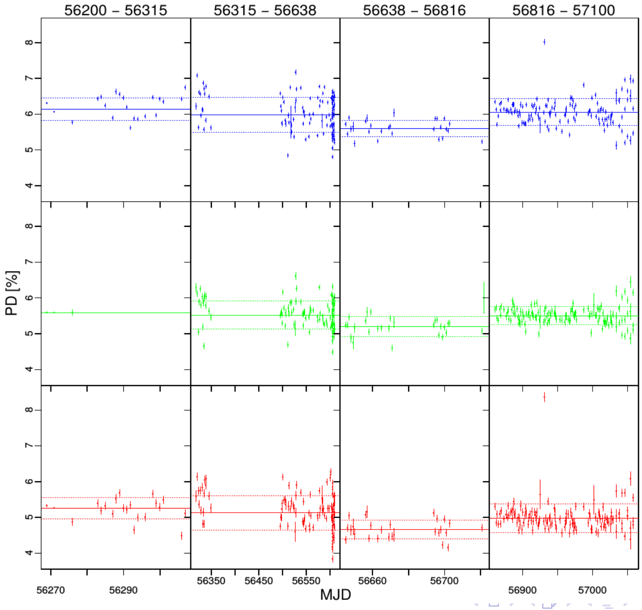

LT/RINGO3 shifts in Q-U plane

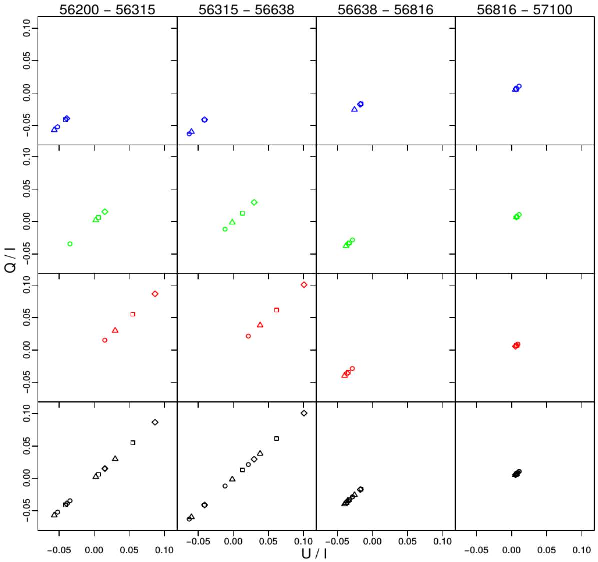

SAX J2103.5+4545

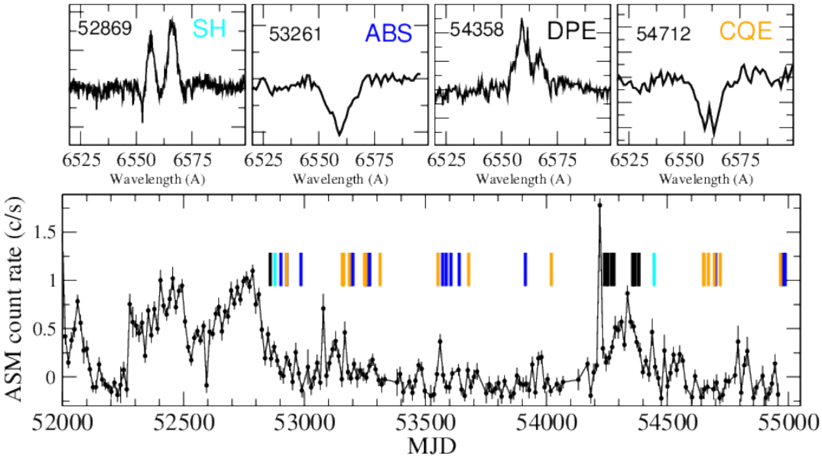

P. Reig, A. Słowikowska, A. Zezas, P. Blay, (2010)

PD for different orbital parameters

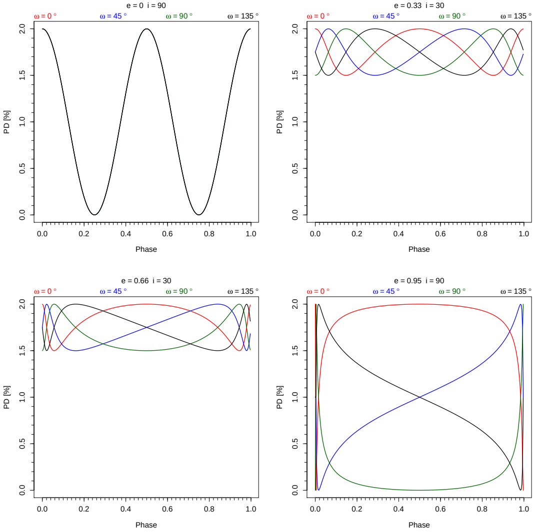

$$p = p_{max}(1 - \sin^2 i \cdot \sin^2(\omega + \nu)),$$

Harries and Howarth, 2000

PD for different orbital parameters

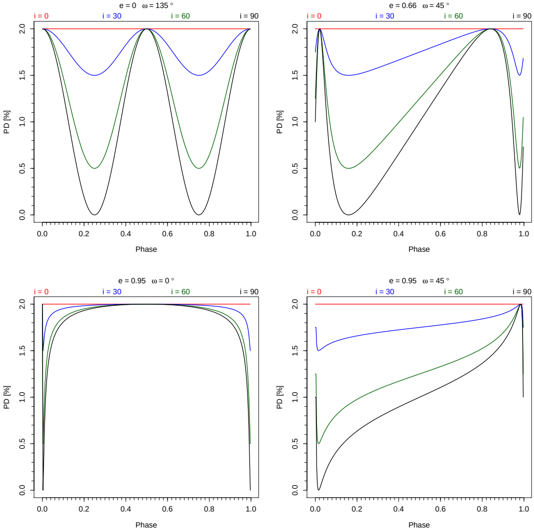

$$p = p_{max}(1 - \sin^2 i \cdot \sin^2(\omega + \nu)),$$

Harries and Howarth, 2000

PD for different orbital parameters

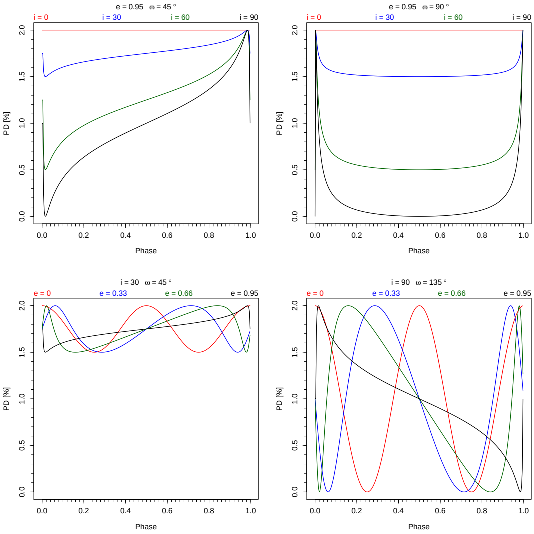

$$p = p_{max}(1 - \sin^2 i \cdot \sin^2(\omega + \nu)),$$

Harries and Howarth, 2000

LT/RINGO3 observations of the SAX J2103.5+4545

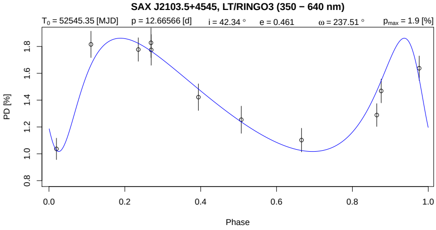

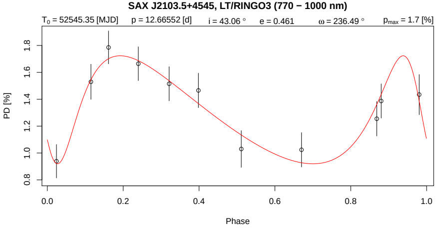

$$p = p_{max}(1 - \sin^2 i \cdot \sin^2(\omega + \nu)),$$

Harries and Howarth, 2000

Orbital parameters of SAX J2103.5+4545

	BLUE (350-640 nm)	RED (770-1000 nm)
T0 [MJD]	52545.351 $\pm$ 37.517	52545.351 $\pm$ 31.079
P_{orb} [days]	12.665663 $\pm$ 0.101095	12.665517 $\pm$ 0.0838
i [deg]	42.34 $\pm$ 2.96	43.06 $\pm$ 2.57
e	0.461 $\pm$ 0.040	0.461 $\pm$ 0.032
ω [deg]	237.51 $\pm$ 6.03	236.49 $\pm$ 4.89
p_{max} [%]	1.86 $\pm$ 0.07	1.72 $\pm$ 0.05
χ^2	8.7	2.79
χ^2_{red}	2.2	0.7

SAX J2103.5+4545 mass function